JOURNAL OF MATERIALS SCIENCE 26 (1991) 4455–4460

Acoustic emission as a technique to study breakaway oxidation and spalling behaviour of 2.25Cr–1Mo steel

B. B. JHA*, BALDEV RAJ*, A. S. KHANNA‡, D. K. BHATTACHARYA*
** Division for PIE and NDT Development, and ‡ Metallurgy Division, Indira Gandhi Centre for Atomic Research, Kalpakkam 603 102, India*

K. J. L. IYER
Metallurgical Engineering Department, Indian Institute of Technology Madras, Madras 600 036, India

The onset of breakaway oxidation and cracking of the oxide scale formed on 2.25Cr–1Mo steel in air at 1173 K have been studied by the acoustic emission (AE) technique. AE parameters, i.e. events, ring-down counts, rise time, event duration and root mean square voltage show negligible increase during isothermal heating at this temperature, until a point where a sudden increase in AE activity is found. This point corresponds to the onset of breakaway oxidation. An enormous increase in AE activity after the start of cooling from the oxidation temperature has been attributed to separation of the oxide scale from the matrix. The peak amplitude distribution is measured and a derived *b* parameter is calculated. This has helped in distinguishing the phenomena of isothermal oxidation at 1173 K and internal cracking of oxide scale during cooling from 1173 K.

1. Introduction

The acoustic emission (AE) technique has been used to study the oxidation behaviour of some ferritic steels [1–5]. The AE count rate or cumulative AE count rate is the parameter that has been used by several workers to measure the scale cracking as a function of time [1, 3–5]. In our previous study [1], AE counts, AE event counts and r.m.s. voltage level have been used to detect the breakaway phenomenon and internal cracking of oxide scale in 2.25Cr–1Mo steel. Frequency analysis of the AE signal was also utilized to differentiate the breakaway phenomenon during isothermal oxidation and internal cracking of the scale during post-oxidation cooling [2]. There are certain other time-domain parameters which give information regarding spalling and internal cracking taking place during oxide growth. The rise time and event duration of the AE signal are two such parameters which can provide valuable information in addition to that obtained from more widely used parameters such as AE event or count rate analysis. In addition, amplitude distribution analysis holds promise in characterizing the AE signals obtained during a real-time isothermal oxidation test. The slope of the logarithmic cumulative amplitude distribution plot, which gives a derived *b* parameter, can indicate a change in the severity of the source mechanisms [6].

Due to the complex nature and the difference in appearance of AE signal waveforms, a number of parameters are used when AE test data are presented. The most common parameters are based on ring-down counting measurements, where the number of times a threshold voltage is crossed by the signal output caused by AE is counted. Fig. 1 shows various parameters associated with AE signal ring-down counts. As discussed above, the most common parameters used in characterizing AE are cumulative events or counts. However, recently, increasing importance has been given to parameters such as rise time, event duration and peak amplitude. The signal rise time is defined as the time period between the time when the AE signal is first detectable above the threshold level and the time when the peak amplitude occurs. Event duration is defined as the length of time during which the burst signal is detectable. Measurement of these parameters along with the peak amplitude distribution can be useful in characterizing AE signals [7].

Recently Sklarczyk and Waschkies [8] have used rise time and event duration to detect and assess defects in reactor pressure components like vessels and pipes during hydrotest and in service. The preference for rise time compared with the other signal parameters is due to the fact that rise time reflects the source lifetime, at least in the near field. Based upon observations, it was concluded that small rise times are related to crack growth and longer rise times are related to crack surface interference. Chelladurai *et al.* [9] have used rise time, peak amplitude and event duration for developing a simple acceptance criterion for the integrity assessments of pressurized systems. Botten [10], while evaluating the characteristics and

0022–2461/91 $03.00 + .12

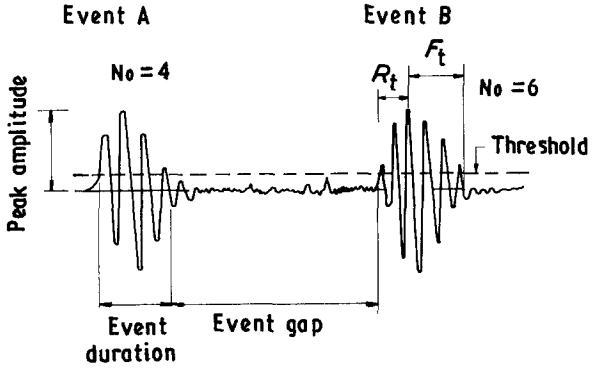

Figure 1 Various parameters of acoustic emission signals. R_t = rise time, F_t = fall time; no. of ring-down counts = 4 (event A) and 6 (event B).

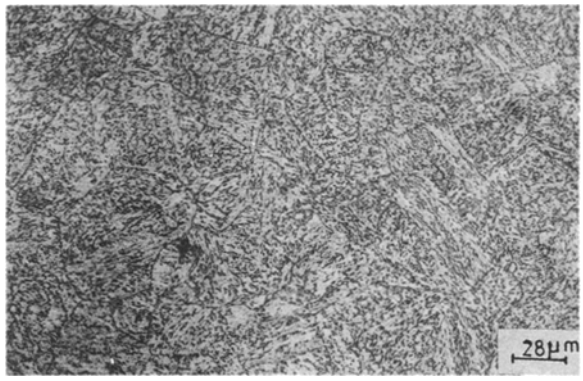

Figure 2 Optical micrograph showing microstructure of normalized 2.25Cr–1Mo steel.

source of AE bursts emitted by material during failure, has brought out the discrepancies arising from measuring only selective AE parameters. The need for measuring rise time and event duration is emphasized in these results.

Amplitude distribution analysis commonly uses the peak amplitude of an AE burst as the amplitude parameter. The relationship between the cummulative AE events and peak amplitude is often given by a power law of the form [11]

$$F(V) = (V/V_0)^{-b}$$

where V_0 is the lowest detectable amplitude and b is a constant. A lower value of b indicates a signal showing a large number of high-amplitude events, while a higher value of b signifies a signal having a large number of small-amplitude events. The b parameter is used to characterize the phenomenon responsible for AE generation.

In the present work, the relationships of AE parameters and the oxidation process of 2.25Cr–1Mo steel are highlighted. Oxidation was carried out at 1173 K. The study aims to characterize the phenomenon of breakaway oxidation and internal cracking during post-oxidation cooling. The temperature of 1173 K was selected since at this temperature both the phenomena take place and the test can be concluded within a reasonably short time period. Time-domain AE parameters, namely rise time and event duration along with events, ring-down counts and r.m.s voltage, have been used to assess the dynamic oxidation process. Amplitude distribution analysis has been used to differentiate the phenomenon of breakaway oxidation from internal cracking of the oxide scale.

2. Experimental procedure

The material, i.e. 2.25Cr–1Mo ferritic steel with C–0.07 wt % was in the form of 6 mm thick sheets in the as-received condition. Strips of such sheets with dimensions of 10 mm × 100 mm were cold-rolled to a final thickness of 1 mm, and sealed in evacuated (10^{-6} torr) quartz tubes. They were then given normalizing treatment at 1223 K for 2 h. Coupons of size 10 mm × 10 mm cut from these strips and polished up to a fine diamond finish (2 μm) were used for the

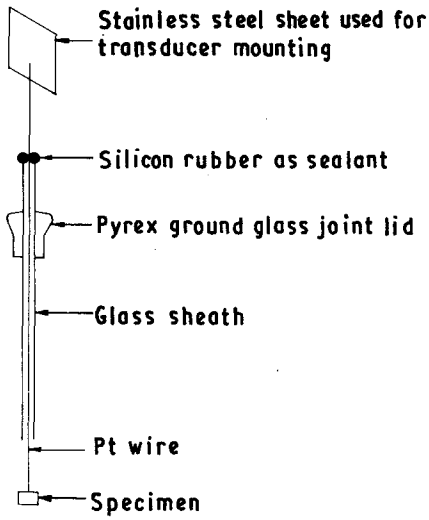

Figure 3 Schematic diagram of the waveguide. Pt wire diameter = 1 mm; specimen 10 mm × 10 mm × 1 mm.

experiments. Typical microstructure of the normalized specimen is shown in Fig. 2.

There was no significant change in the experimental set-up for measuring the additional AE parameters like rise time and event duration as compared to the set-up used for event and ring-down count measurement reported earlier [1]. An inert platinum wire was used for the waveguide. Platinum has very low attenuation for the AE signal and has very high oxidation resistance. The wire, of 1 mm diameter and 0.5 m in length, was spot-welded to the specimen at one end and to a stainless steel plate at the other end of the wire. The integral assembly of the platinum wire and stainless steel plate acted as the AE waveguide (Fig. 3). AE monitoring was carried out using the AET-5000 system manufactured by Acoustic Emission Technology Corp. (USA). A piezoelectric transducer with a resonant frequency of 175 kHz (filter 125–250 kHz) was used. A total system gain of 96.4 dB and threshold voltage 0.7 V was maintained throughout. A dummy run was carried out without spot-welding the specimen to the platinum wire with the same threshold voltage and gain value. It was then ensured that no extraneous spurious signal was recorded during the oxidation test. A schematic diagram of the experimental set-up is shown in Fig. 4. For thermogravi-

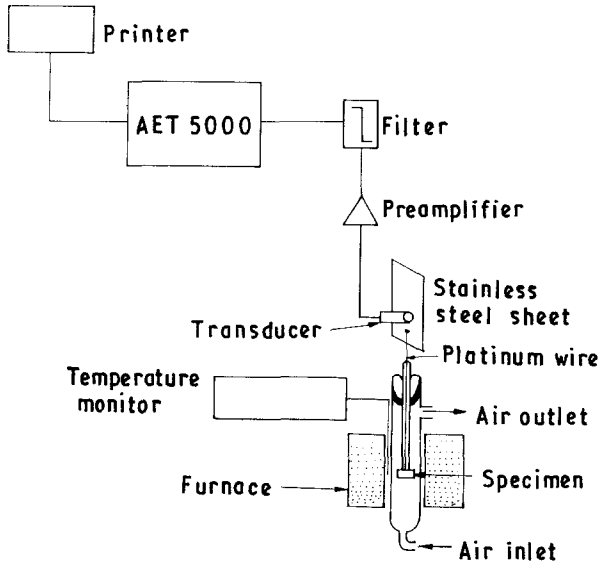

Figure 4 Schematic diagram of the experimental set-up.

metry studies, a Metller TA1 thermoanalyser was used. The balance system had a sensitivity of 0.005 mg.

3. Results

The variations in rise time (R_t) and event duration (E_d) plots corresponding to the isothermal oxidation of 2.25Cr–1Mo steel at 1173 K are shown in Fig. 5 along with the variation in events and ring-down counts. The sudden increase in AE activity at point C (105 min) during isothermal oxidation at 1173 K, resulting in a higher rise time (Fig. 5a) and event duration (Fig. 5b), indicates that the characteristics of AE pulses generated in this region are different from those of pulses generated during the time preceding the point C. The increase in AE activity at point C is due to the occurrence of breakaway oxidation; this is confirmed by the thermogravimetry results shown in Fig. 6, in which point X denotes the breakaway point. It is to be noted that the breakaway oxidation point as detected by AE is 15 min earlier than that detected by thermogravimetry results, illustrating the sensitivity of the AE technique for the detection of breakaway oxidation.

Rise time and event duration plots obtained during cooling of the oxidized samples from 1173 K are shown in Fig. 7 along with events and ring-down counts. The higher AE activity during cooling (Fig. 7c and d) as compared to that during isothermal oxidation (point C Fig. 5c and d) may be noted. AE pulses are also of very high rise time and event duration (Fig. 7a and b).The generation of large acoustic emissions of higher rise time and event duration was found to be due to internal cracking and/or separation of the scale from the matrix. The separation between the inner and outer layers of the oxide scale was also observed (Fig. 8).

The r.m.s. voltage of the AE signal obtained during isothermal oxidation and averaged for 1 s is shown in Fig. 9a. This figure indicates the presence of a burst of AE at the 105th minute of isothermal oxidation corresponding to point C of Fig. 5. The r.m.s. voltage level plot of the AE signal obtained during cooling of the oxidized samples is shown in Fig. 9b. Comparing the r.m.s. voltage level plots, it is clear that the strength of AE is higher during cooling than that obtained during isothermal oxidation after breakaway.

Fig. 10 shows the peak amplitude distribution of the AE signal obtained during isothermal oxidation and during cooling. The large difference in peak amplitudes of AE signals generated during the two different phenomena is noteworthy. Fig. 11 compares the logarithmic cumulative amplitude distribution plots of the AE signal obtained during isothermal oxidation and during cooling from 1173 K. The distribution obtained during cooling shows a double-slope behaviour having a power-law exponent (the b parameter) of 0.95

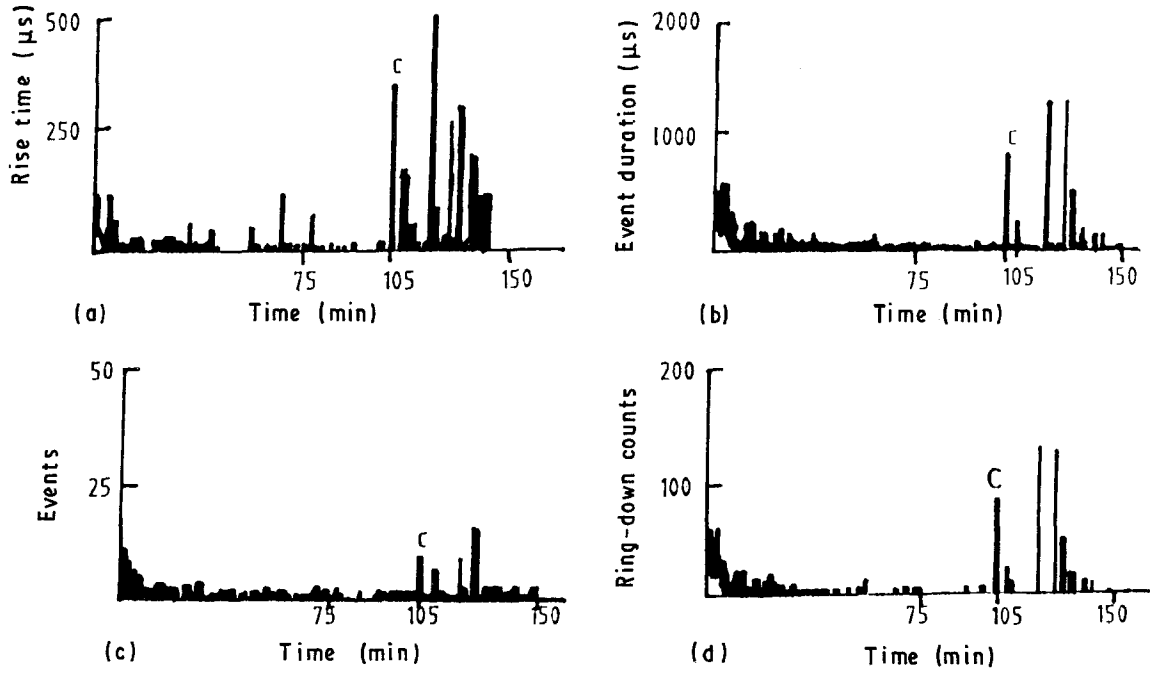

Figure 5 Various acoustic emission parameters obtained during isothermal oxidation at 1173 K. Point C = start of breakaway oxidation.

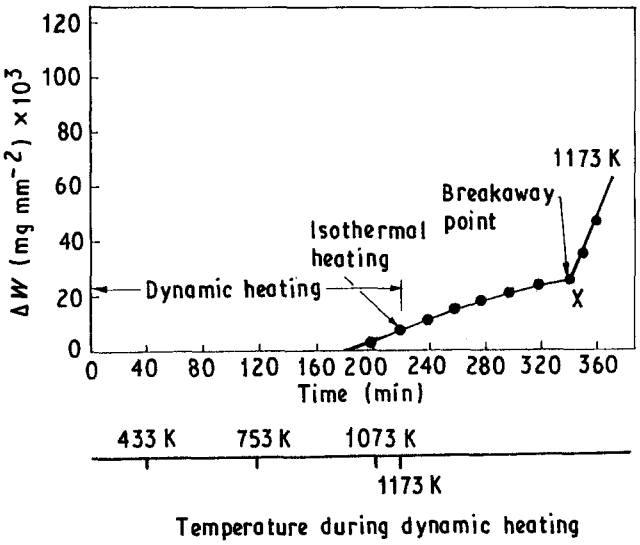

Figure 6 Thermogravimetric weight gain plot during oxidation of 2.25Cr–1Mo steel in air at 1 atm pressure.

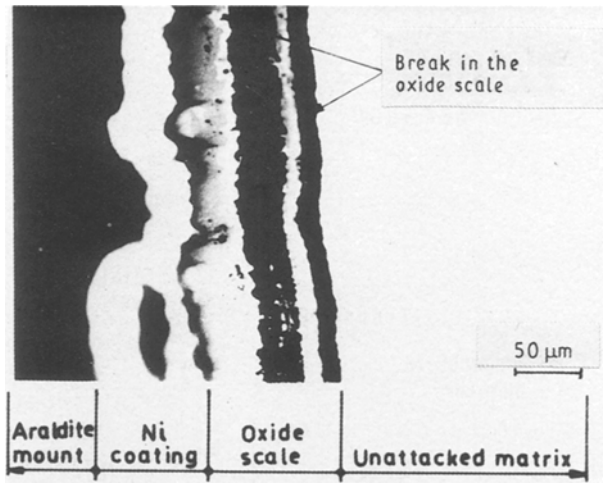

Figure 8 Cross-section of the oxide scale formed on 2.25Cr–1Mo steel at 1173 K, indicating cracking in the oxide scale.

in the lower-amplitude region and 2.3 in the higher-amplitude region. The parameter obtained for the breakaway oxidation region is found to be 2.5.

4. Discussion

The phenomenon of breakaway oxidation is associated with microcracking of the oxide scale [12]. This leads to higher oxidation rates. The present work has shown that such microcracks can be detected sensitively by the AE technique by measuring the significant increase in AE parameters such as events, ring-down counts, rise time, event duration and r.m.s. voltage level. On comparing the AE results with thermogravimetry results, it emerged that the AE technique detects the onset of breakaway oxidation earlier than the thermogravimetric technique. The phenomenon of breakaway on AE-tested specimens was confirmed by observation of the surface topography of the oxide layer. A large increase in AE activity as well as in its r.m.s. voltage level during post-oxidation cooling was found to be due to separation of oxide scale from the matrix.

The significant increase in the rise time and event duration of AE pulses during breakaway oxidation and cooling could be due to the following causes: (i) an increase in the value of the strength of AE signals, and/or (ii) an increase in the time durations of the source mechanisms generating AE signals. It is seen in the r.m.s. voltage level plots that the strength of AE is greater when it is generated during post-oxidation cooling. The peak amplitude distribution plots of these two regions also indicate a similar trend. An increase in the peak amplitude has contributed to the increase in the rise time and event duration of AE signals generated during cooling. The increased values may also be a manifestation of the source mechanisms having higher time durations. This is evident from the

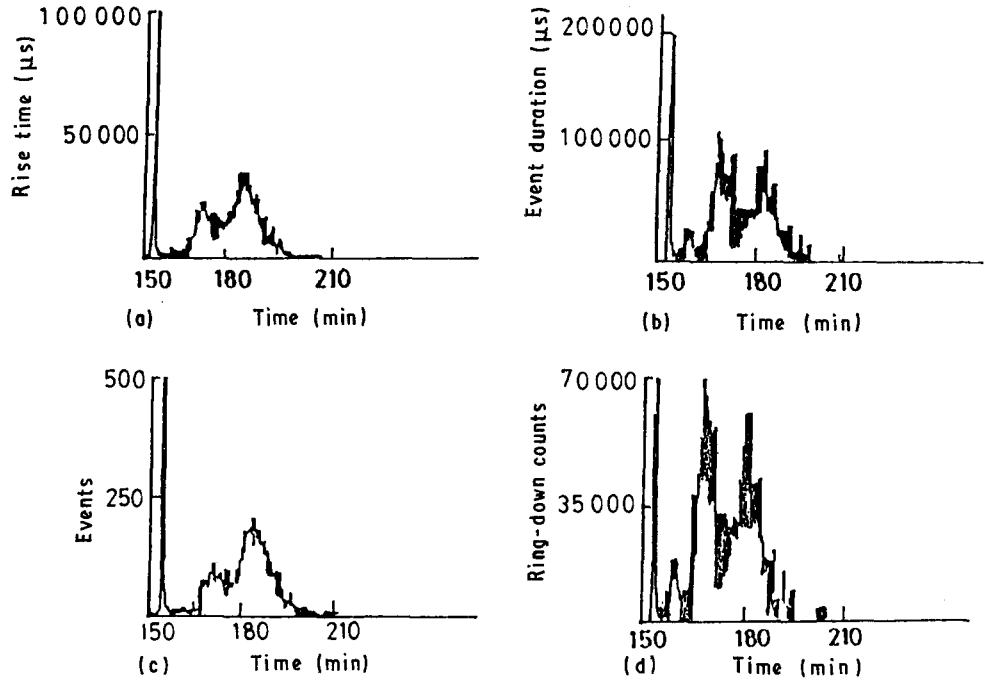

Figure 7 Various acoustic emission parameters obtained during cooling from 1173 K.

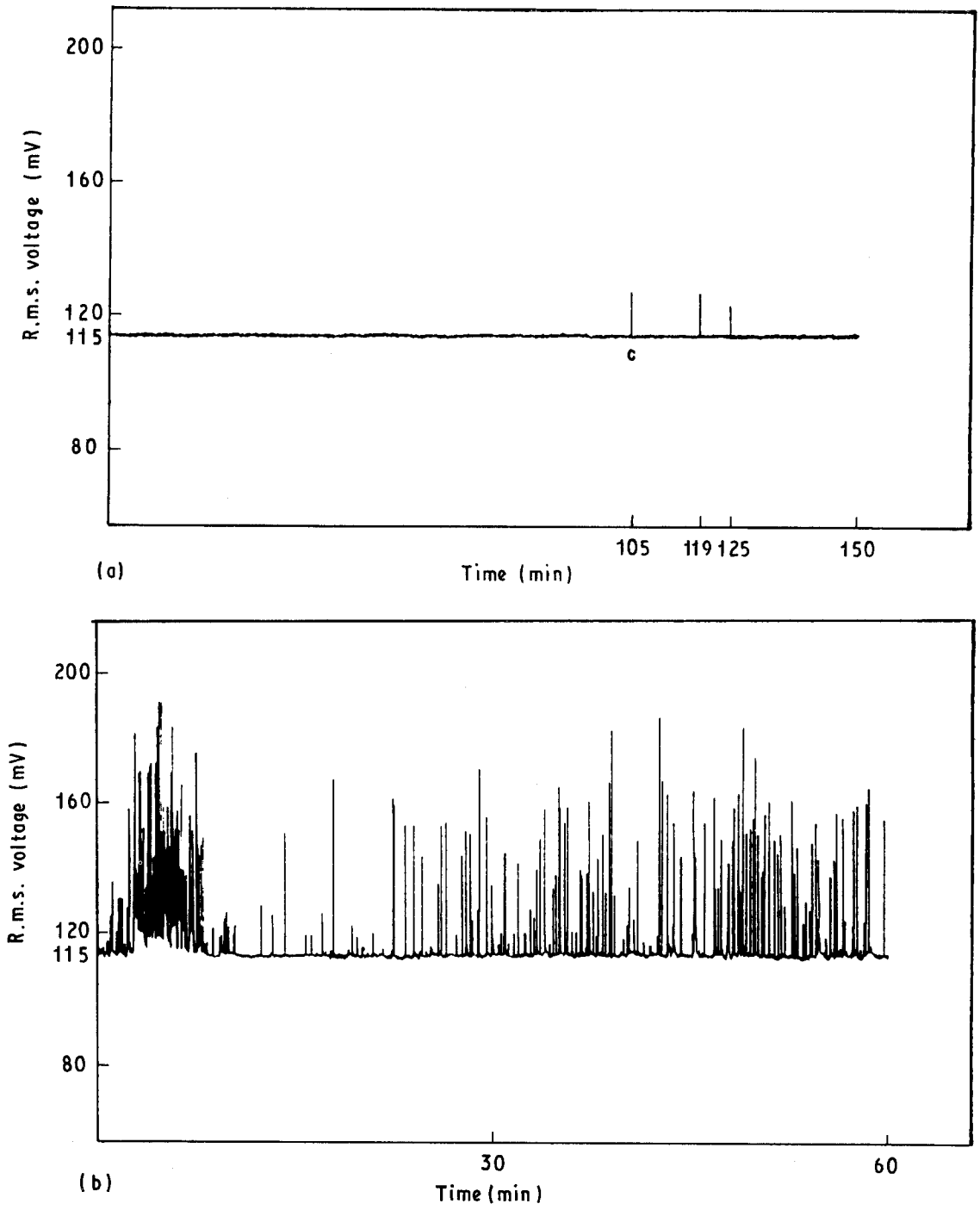

Figure 9 R.m.s. voltage plot of AE signal obtained (a) during isothermal oxidation at 1173 K and (b) during cooling from 1173 K. C = start of breakaway oxidation.

slopes of the AE pulses for these two regions. The slope of AE pulses calculated at the most abundant peak amplitude is found to be orders of magnitude higher in the breakaway oxidation region (5.6×10^{-2} dB μs^{-1}) than in the internal cracking region (8.8×10^{-4} dB μs^{-1}). These differences show that the characteristics of the pulses of AE for these two regions are different. In one case, it is taking place in smaller time durations and in the other case in larger time durations. Our results based on frequency analysis reported earlier [2] also support the more transient nature of the source characteristics responsible for generating AE during breakaway oxidation region, as compared to the source characteristics of AE generation during internal cracking.

There exists a large difference in the nature of the peak amplitude distribution plots of AE events generated during isothermal heating and those during cooling from 1173 K. The cut-off peak amplitude of the AE observed during isothermal heating (i.e. the value beyond which there is no AE event) is 30 dB, whereas the same for cooling is extended up to 65 dB. The derived parameter, i.e. the b-parameter, is also useful in distinguishing the breakaway oxidation and internal cracking processes. A large value of b represents a phenomenon dominated by low-energy emissions, while a small value of b represents the dominance of high-energy emissions. The calculated b value obtained for isothermal heating is 2.5 and the same for cooling is represented by 0.95 in the lower-

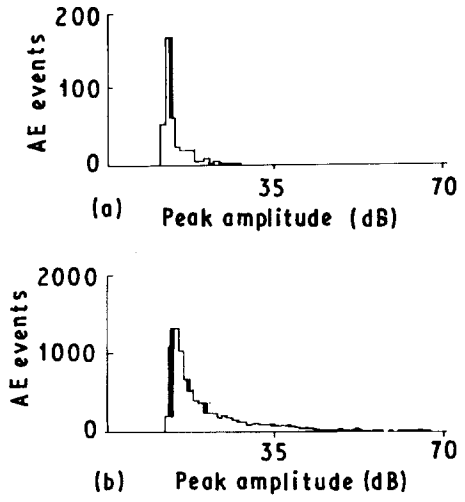

Figure 10 Peak amplitude distribution of AE events (a) during isothermal oxidation at 1173 K (b) during cooling from 1173 K.

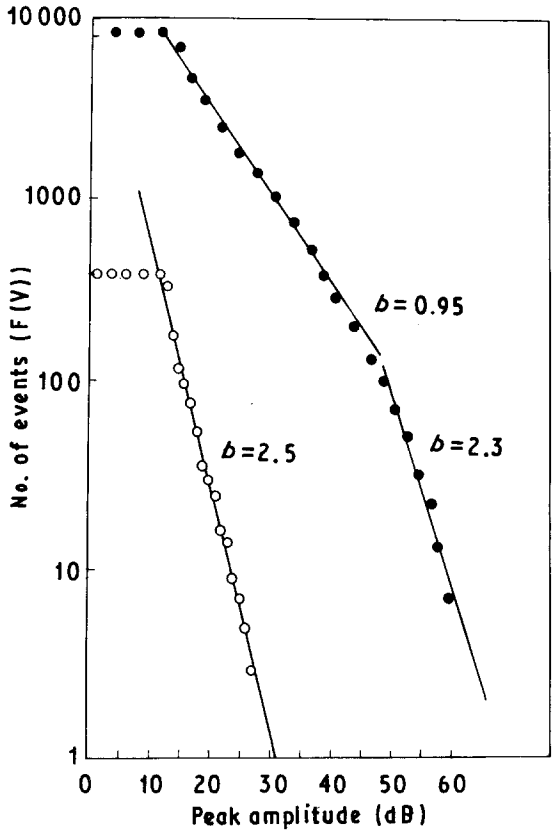

Figure 11 Logarithmic cumulative amplitude distribution plots of the AE signal obtained (○) during isothermal oxidation and (●) during cooling from 1173 K.

amplitude region and by 2.3 in the higher-amplitude region. This exponent of 2.3 being closer to the value of 2.5 indicates that the source mechanism responsible for AE generation during cooling is initially similar to that taking place at breakaway oxidation. As the process proceeds more intense AE is generated, shifting the value of b to a lower value.

5. Conclusions

The acoustic emission technique successfully detects on-line occurrence of breakaway oxidation and is capable of giving additional information related to dynamic changes in the material and the oxide scale. The additional information cannot be obtained by thermogravimetry and microstructural studies. Since microcracking in the oxide scale precedes by a considerable time the observation of weight gain, the AE technique detects the breakaway point earlier than the thermogravimetry method. Among the two processes studied, i.e. microcracking at the onset of breakaway oxidation and the internal cracking during cooling, the latter is more energetic and takes place with larger time durations. This was established on the basis of the analysis of r.m.s. voltage level, rise time and event duration of the AE signal. The value of the b-parameter obtained through amplitude distribution analysis was found to be able to characterize the phenomena of internal cracking of the oxide scale observed during cooling and microcracking of the oxide scale during breakaway oxidation.

Acknowledgements

The authors thank Dr Placid Rodriguez, Head, Metallurgy and Materials Programme for his constant encouragement and support during the course of this study. They also thank Shri P. Kalyanasundaram, Head, Signal Processing and Electronics Section for many useful discussions.

References

1. A. S. KHANNA, B. B. JHA and BALDEV RAJ, *Oxid. Metals* **23** (1985) 159.
2. B. B. JHA, BALDEV RAJ and A. S. KHANNA, *ibid.* **26** (1986) 263.
3. A. S. KHANNA, B. B. JHA and BALDEV RAJ, *ibid.* **27** (1987) 97.
4. B. B. JHA, A. S. KHANNA and BALDEV RAJ, *J. Mater. Sci.* **22** (1987) 2823.
5. W. CHRISTL, A. RAHMEL and M. SCHUTZE, *Mater. Sci. Engng* **87** (1987) 289.
6. BALDEV RAJ, PhD thesis, Indian Institute of Science, Bangalore (1989).
7. A. G. BEATTIE, *J. Acoust. Emission* **2** (1983) 95.
8. C. SKLARCZYK and E. WASCHKIES, *ibid.* **8** (1989) S330.
9. T. CHELLADURAI, R. KRISHNAMOORTHY and A. R. ACHARYA, *ibid.* **8** (1989) S88.
10. S. F. BOTTEN, *ibid.* **8** (1989) S330.
11. A. A. POLLOCK, *NDT Internat.* **6** (1973) 264.
12. G. C. WOOD and D. P. WHITTLE, *Corros. Sci.* **7** (1967) 763.

Received 1 June 1990
and accepted 15 January 1991